

Research Article

Cassava Starch-Based Multifunctional Coating Incorporated with Zinc Oxide Nanoparticle to Enhance the Shelf Life of Passion Fruit

Han Congying,¹ Wang Meifang,¹ Md. Nahidul Islam ,^{2,3} Shi Cancan,¹ Guo Shengli,¹ Afsana Hossain ,⁴ and Cao Xiaohuang ^{1,5,6}

¹College of Chemistry and Food Science, Yulin Normal University, Yulin 537000, China

²Department of Agro-Processing, Bangabandhu Sheikh Mujibur Rahman Agricultural University, Gazipur 1706, Bangladesh

³Institute of Food Safety and Processing, Bangabandhu Sheikh Mujibur Rahman Agricultural University, Gazipur 1706, Bangladesh

⁴Department of Plant Pathology, Bangabandhu Sheikh Mujibur Rahman Agricultural University, Gazipur 1706, Bangladesh

⁵School of Food Technology, Guangdong Ocean University, Zhanjiang, China

⁶Guangxi Key Laboratory of Agricultural Resource Chemistry and Biotechnology, Yulin, China

Correspondence should be addressed to Md. Nahidul Islam; nahidul.islam@bsmrau.edu.bd
and Cao Xiaohuang; caoxh@ylu.edu.cn

Received 20 December 2023; Revised 22 April 2024; Accepted 27 April 2024; Published 14 May 2024

Academic Editor: Yogesh Kumar

Copyright © 2024 Han Congying et al. This is an open access article distributed under the Creative Commons Attribution License, which permits unrestricted use, distribution, and reproduction in any medium, provided the original work is properly cited.

Passion fruits are susceptible to numerous postharvest challenges including weight loss, ethylene production, peel shrinkage, microbial growth, and pulp liquefaction. To mitigate these issues, yellow passion fruits were treated with hydroxypropyl cassava starch zinc oxide (HCS-ZnO) nanoparticles at varying concentrations. Fruits were stored at 10°C for 42 days, and the treated fruits underwent periodic assessments for weight loss, electrical conductivity, reducing sugar, total soluble solids (TSS), titratable acidity, and peel color. The results showed that a 0.8% HCS-ZnO nanoparticle coating could significantly reduce the weight loss of passion fruit during storage. However, compared to other treatments, a 0.2% HCS-ZnO nanoparticle coating demonstrated superior preservation of physicochemical properties, delayed discoloration, slowed ripening, maintained cell membrane integrity (electrical conductivity 1337 $\mu\text{s}/\text{cm}$), and reduced nutrient loss (titratable acidity 3.35 g/100 mL, TSS 17.9%, reducing sugar 5.1 g/100 g) at 42 days of storage. This innovative approach holds promise for commercial application, offering a sustainable solution to mitigate postharvest losses of passion fruit. The study underscores the potential of HCS-ZnO nanoparticles as effective coatings to uphold fruit quality and extend shelf life, presenting compelling insights for future fruit preservation strategies.

1. Introduction

Passion fruit (*Passiflora edulis* Sim.) belongs to the family *Passifloraceae* and is a shrub or herbaceous plant, mostly climbing in nature with auxiliary tendrils [1]. Currently, Guangxi has emerged as China's primary hub for passion fruit cultivation, boasting a plantation area exceeding 20,000 hectares. The total yield across Guangxi has reached approximately 300,000 tons. Notably, around 80% of this yield is directed to the fresh food market. Moreover, there has been a consistent upward trend in the average selling

price of passion fruit [2]. Since passion fruit is climacteric in nature with a very high metabolism, the major problems encountered by the farmers during the storage of passion fruits are increased respiratory rate, massive water loss, quick browning of peel, etc., which seriously deteriorate the quality of passion fruit and greatly limit its shelf life [3]. During postharvest storage at room temperature for 30 days, passion fruit showed higher metabolic and physiological processes [4]. These processes led to higher weight loss, peel shrinkage, microbial infection, and pulp liquefaction [5]. It is, therefore, essential to find a sustainable solution

to preserve the quality and enhance the shelf life of passion fruits.

Harvesting at the right maturity level is one of the prerequisites that determines the postharvest quality of passion fruit. Several novel technologies have been applied to enhance the storage potential of various fruits and vegetables [6–8]. Modified atmosphere storage by increasing CO₂ concentrations, lowering O₂ concentrations, and removing ethylene is one of the most common practices. However, the storage gas composition regulation requires expensive engineering work, which increases storage and transportation costs, and the byproducts from these systems are not environmentally friendly [9]. Low-temperature (nonfreezing) storage is another way of extending shelf life. At subzero freezing points above the range of frozen storage, the tissue cells of fruits and vegetables remain alive and do not cause postharvest chilling injury or damage to cell structure [10, 11]. Furthermore, low-temperature storage requires a significant amount of energy, which increases storage and transportation costs [12].

By preventing microbiological deterioration and acting as a barrier against moisture and gas, nanoparticle-based coatings become a cutting-edge method of food preservation that can maintain the quality of fruits and vegetables and increase their shelf life [13–15]. Among inorganic substances, ZnO stands out due to its notable appeal, attributed to the safety it offers for both animals and humans [16]. The Food and Drug Administration (FDA) in the United States has granted approval for ZnO as a safe substance, endorsing its wide-ranging utilization in drug delivery, pharmaceuticals, food supplements, and other fields [17]. ZnO nanoparticle edible coating has been applied recently to maintain the quality of fresh-cut mangoes [18], bananas [19], avocados [20], and various climacteric fruits [21]. Recently, dos Santos Junior et al. [22] applied resin and zinc oxide nanocomposites to chitosan coatings to extend the shelf life of passion fruits. They kept passion fruits for 10 days at 22.5°C and found them effective in maintaining quality.

Starch-based biocomposite films gained popularity for maintaining the quality of fruits and vegetables due to their low price, wide availability, and overall performances [23–25]. No study has been carried out to enhance the shelf life of passion fruits by applying starch-based nanoparticle coating. Therefore, the aim of the study was to evaluate the potential of the novel cassava starch-based multifunctional coating containing zinc oxide nanoparticles to enhance the shelf life of passion fruit by reducing water and nutrient loss, alleviating deterioration of quality during storage, and maintaining overall freshness. This study used cassava starch, a natural edible macromolecule capable of forming a cohesion structure, as the coating matrix, incorporating nano-ZnO at varying concentrations.

2. Materials and Methods

2.1. Materials. The yellow passion fruit was collected from an orchard in Yulin, China (110.17°E, 22.63°N, cultivated in August–November 2021). The fruits were harvested at a physiologically mature stage (75% color turning). 25 kg of

fruits with similar size, shape, and absence of disease incidence were then brought to the laboratory of Food Science at Yulin Normal University within 2 hours of harvest. All the required chemicals were analytical grade and were purchased from Sinopharm (Shanghai, China). The overview of the experiment is presented in Figure 1.

2.2. Preparation of Cassava Starch ZnO Nanoparticles. ZnO solution (0.5 M) was prepared by dissolving ZnO (4.07 g) (analytical grade, purity ≥ 98%) in ethylene glycol (10 mL) and adding Millipore water to make a volume of 100 mL. ZnO nanoparticle was synthesized using a protocol modified from an earlier study [26]. The prepared ZnO solution was then heated at 180°C for 3 h. The solution was then placed on a magnetic stirrer at 80°C for another 3 hours. The final product after centrifugation (492 g for 15 min) was collected and dried in a vacuum oven at 70°C overnight.

Hydroxypropyl cassava starch (HCS) was prepared by esterification of cassava starch (supplied by Sinopharm Chemical Reagent Co., Ltd., Shanghai, China) and propylene oxide under alkaline conditions, as described by Phinainitsatra et al. [27]. HCS (2.7 g) was heated and pasted with 100 g of distilled water at 90°C. The temperature of the solution was reduced to room temperature, and then 0 g, 0.2 g, 0.4 g, 0.6 g, and 0.8 g dried ZnO nanoparticles were added to it to prepare 0%, 0.2%, 0.4%, 0.6%, and 0.8% HCS-ZnO nanoparticle dispersions, respectively [28]. The dispersion was then homogenized using a homogenizer.

2.3. Application of Nanoparticle Coating to Passion Fruits. Each passion fruit was completely dipped in the prepared dispersion solution (1000 mL) and kept in it for 5 minutes. The experiment used a total of 700 fruits. There were 135 samples in each group. A separate set of 25 total samples (5 in each group) was used for repeated color and weight loss measurements. The coatings were then dried naturally at room temperature on a clean surface. All samples were then stored in a mini cold storage at refrigerated temperature of 10°C and 85% relative humidity (RH), since it is recommended as the optimum storage condition for yellow passion fruits [29]. Control for individual solutions was not studied.

2.4. Characterization of Nanoparticles. UV-visible spectroscopy with a spectrophotometer (UH5300 Spectrophotometer, Hitachi, Japan) was used to identify the formation of ZnO nanoparticles. The spectrophotometer operated from 200 to 800 nm at a resolution of 1 nm. The HCS-ZnO nanoparticle solutions were analyzed by Fourier transform infrared (FTIR) spectroscopy (Perkin Elmer Spectrum Two™, Waltham, USA) in order to identify the functional groups that are responsible for the production and maintenance of ZnO nanoparticles [30]. Perkin Elmer's FTIR software and Peak Fit software (Peak Fit version 4.12, Sea Solve Software Inc. Framingham, USA) were used to interpret the FTIR spectra of the HCS-ZnO nanoparticles [31].

The crystalline nature of ZnO, HCS, and HCS-ZnO nanoparticles (freeze-dried powder) was observed using X-ray Diffraction (XRD) spectroscopy [30]. The mean particle

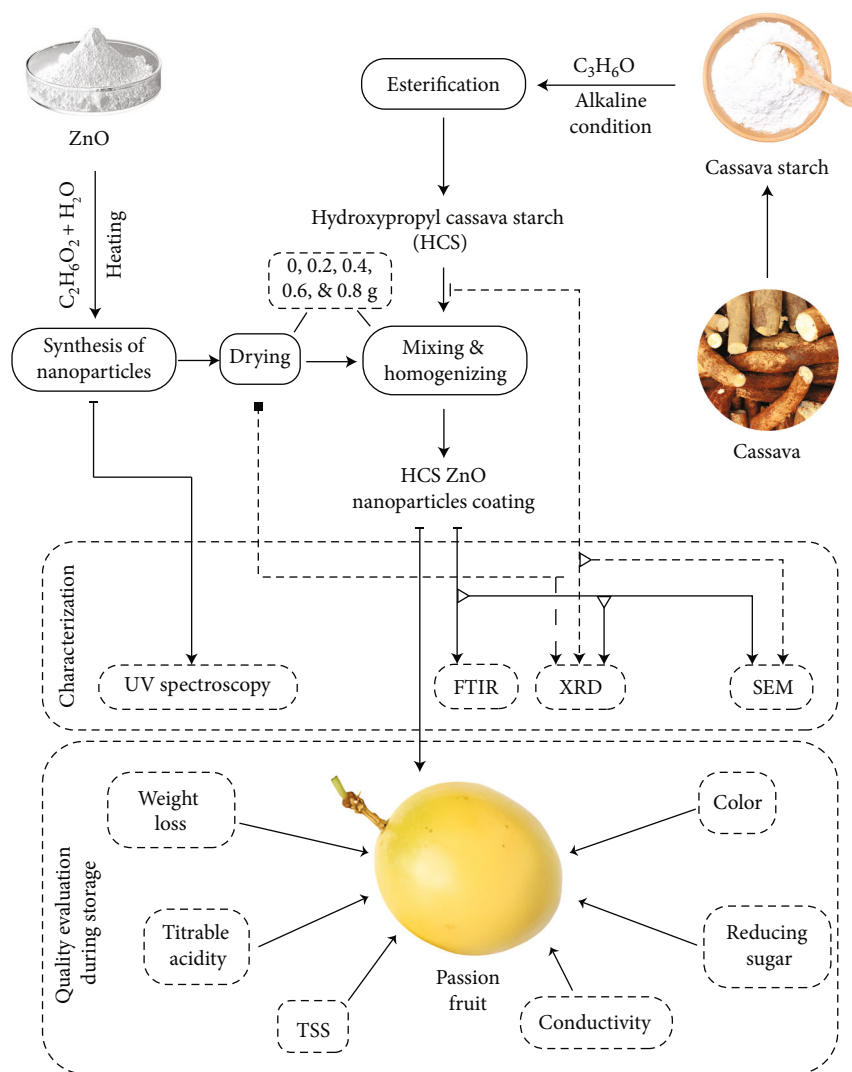


FIGURE 1: Overview of the experimental flow diagram.

size of ZnO nanoparticles was approximated utilizing the Debye–Scherer equation, which establishes a correlation between peak broadening observed in XRD and particle size, as shown by the equation below:

$$D = \frac{k\lambda}{\beta \cos \theta}, \quad (1)$$

where D is the crystal size in nm, k is the Scherer constant (0.9), λ is the wavelength of X-ray sources (0.15406 nm), β is the FWHM (radian), and θ is the peak position (radian). The surface morphology of the cassava starch and HCS-ZnO freeze-dried coating was analyzed using scanning electron microscopy (SU1510, Hitachi High-Tech, Tokyo, Japan), at 15kV by using the method described by Rahman et al. [32]. The dried sample was uniformly put onto a double-sided adhesive tape affixed to aluminum stubs. Following this, the products mounted on the stubs were covered with a layer of gold coating.

2.5. Determination of Weight Loss. Direct weighing method was used to measure the stored weight of passion fruit (accuracy: 0.01 g). Consistency was maintained by repeated measurements of the same passion fruit at each sampling time throughout the experiment. Weight loss due to physiological processes was calculated as the difference between the initial weight and the weight at the time of measurement [33], which was calculated by using equation (2)

$$\text{Weight loss} = \frac{m_0 - m_n}{m_0} \times 100, \quad (2)$$

where m_0 is the initial weight; m_n is the weight after a period of storage.

2.6. Determination of Titratable Acidity. The passion fruits were halved, and the pulp, peel, and seeds were separated. The pulp was then filtered to make fruit juice. Passion fruit juice (5.0 mL) was directly taken and diluted in a 50 mL volumetric flask. 10.0 mL of diluted solution was taken into a 250 mL conical flask, and 2-3 drops of phenolphthalein

indicator were added. A standard solution of 0.1 mol/L sodium hydroxide was titrated until the indicator changed the pale-yellow solution to light red, with 30 seconds of non-fading as the endpoint of the titration. The volume of sodium hydroxide consumed was recorded as the average of the three replicates. A blank experiment was also carried out. Titrable acidity was measured according to Zhou et al. [34] and calculated as shown by using equation (3)

$$TA = \frac{C \times V \times K \times V_0}{m \times V_1} \times 100, \quad (3)$$

where TA is the titratable acidity (g citric acid/100 mL), C is the concentration of standard NaOH solution (mol/L); V is the volume of standard NaOH solution consumed by titration (mL); m is the sample mass (g); V₀ is the total volume of sample dilution (mL); V₁ is the volume of sample liquid absorbed during titration (mL); K, conversion coefficient, based on citric acid, is 0.064.

2.7. Determination of Total Soluble Solids Content. In order to determine the amount of total soluble solids (TSS), an Abbe refractometer was used. Passion fruits were cut along the equator line, the inner pulp was drugged out, and the juice was filtered into a beaker and set aside. A drop of juice was measured with the calibrated refractometer. The average value from three replicate measurements was expressed as a percentage [35].

2.8. Determination of Peel Color. The color values of the passion fruits were measured using a Minolta colorimeter (CR400; Minolta Co., Ltd., Osaka, Japan), as reported by Islam et al. [36]. Sample lightness is represented by the color value L*, which ranges from 100 (white) to 0 (black). Redness is represented by the a* value, and yellowness by the b* value. The apparatus was twice calibrated in accordance with standard procedure prior to measurement. The lens of the colorimeter was placed at three random points at the equator of passion fruit, and data were recorded.

2.9. Determination of Reducing Sugar. The 3,5-dinitrosalicylic acid (DNS reagent) method was used to determine the concentration of the reducing sugars [37]. 0.5 mL of passion fruit juice and 1 mL of DNS (Sigma-Aldrich, St-Quentin-Fallavier, France) were combined. Following homogenization, the mixture was heated for five minutes to 100°C and then for four minutes to -20°C. DNS is converted to 3-amino,5-nitrosalicylic acid in an alkaline environment. The absorbance was determined using the UV-Vis spectrophotometer at 540 nm (UH5300 Spectrophotometer, Hitachi, Japan). For the calibration curve, glucose (Sigma-Aldrich, St-Quentin-Fallavier, France) was utilized [38].

2.10. Determination of Electrical Conductivity. Passion fruit was cut into half, and a scoop of flesh was taken with a stainless-steel spoon. The flesh was handled gently to avoid any damage. The flesh was then placed on a 0.45 μm membrane filter and allowed the drops of juice to accumulate in a beaker. 2.0 mL of juice was taken in a 50 mL beaker and diluted six times with double-distilled water. A WTW Tetra-

Con 325 electrode (Weilheim, Germany) and a WTW inoLab Cond 730 conductometer were used to test conductivity at 22°C. The findings were presented in terms of microsiemens per centimeter (μS cm⁻¹) [39].

2.11. Data Analysis. A one-way analysis of variance (ANOVA) was employed to investigate the statistical significance of the variation in the average values. For the multiple-comparison, Tukey's honest significant difference (HSD) test was performed using R statistical software (v. 3.1.0, R Foundation, Vienna, Austria). The graphs were created using OriginLab Pro (OriginLab Corporation, Roundhouse Plaza, Suite 303 Northampton, Massachusetts, USA) [40]. Three measurements were made for each. Principal component analysis was carried out with autoscaled data to explore the data in PLS_toolbox under Matlab environment (PLS_toolbox 8.92, Eigenvector Research Inc., USA) [41].

3. Results and Analysis

3.1. Characterization of HCS-ZnO Nanoparticles. In the 350–420 nm range, ZnO nanoparticles revealed a characteristic surface plasmon resonance peak at 388 nm (Figure 2(a)) as assessed by ultraviolet-visible spectroscopy. The primary absorption bands of the Zn–O bond are visible around 575 cm⁻¹ in the HCS-ZnO nanoparticles' FTIR spectra (Figure 2(b)) [42, 43], about 3437 cm⁻¹, the O–H stretching of alcohol and R–COOH and the N–H stretching of amine, alkane, and aldehyde C–H stretching at about 2925 cm⁻¹, C=C stretching N–H bending of alkene and amine at around 1598 cm⁻¹, O–H bending of alcohol at around 1383 cm⁻¹, and minor absorption bands of C=C bending about 750–850 cm⁻¹. The absorption bands other than the Zn–O bonds in the FTIR spectra of ZnO nanoparticles appeared in the FTIR spectrum (Figure 2(b)), indicating that the functional groups on the nanoparticles are from HCS-ZnO nanoparticles.

As shown in Figure 2(c), starch particles, ZnO nanoparticles, and composite coatings have different XRD patterns. 2θ includes 31.73, 34.36, 47.20, 56.52, 62.75, 66.29, 68.85, and 68.99. The positions of these peaks indicate that the metal oxides are ZnO particles and have the XRD characteristics of ZnO. The peaks of ZnO particles appeared in the same position as the HCS-ZnO coating, and the changes in the peak intensity were the same as the characteristics of ZnO. These characteristics indicate that nano-ZnO particles are present in the composite coating. There is only a sharp peak but no flat peak in ZnO particles, which indicates that ZnO exists as a crystal. Flat and sharp peaks appeared in the composite coating, indicating the presence of metal oxide crystals and starch-amorphous areas. This result indicates that the starch crystallized in the composite coating was gelatinized into amorphous material [44]. However, cassava starch has a flat peak and hump, which indicate that it has a crystallization zone and an amorphous zone. The reason is that the peaks are formed by the crystallization of the compounds into crystals, whereas amorphous substances can only produce broad peaks (flat peaks). These characteristics

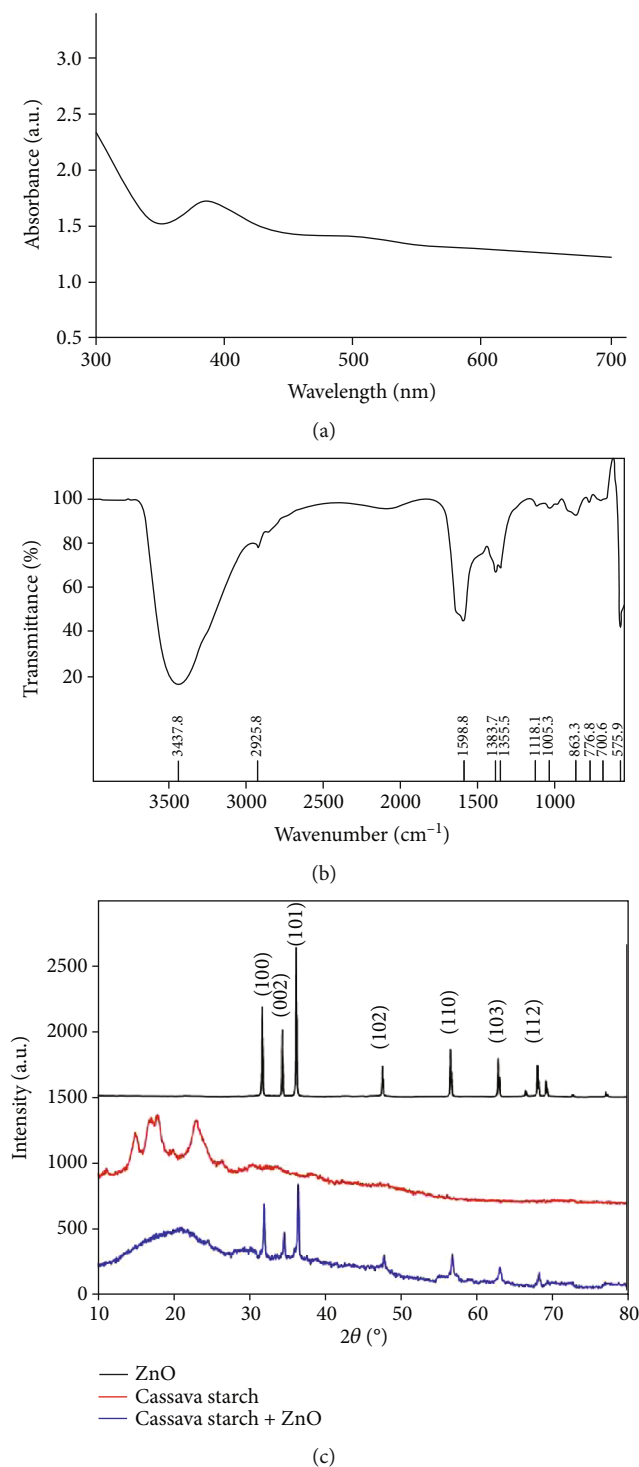


FIGURE 2: (a) Ultraviolet-visible absorption spectrum of the colloidal 0.2% ZnO nanoparticles. (b) Fourier transform infrared spectrum detecting groups in the 0.2% cassava starch ZnO nanoparticles solution. (c) X-ray diffraction pattern indicating crystalline wurtzite structures of the 0.2% ZnO nanoparticles.

have been reported in the most relevant literature [45]. As shown in Figure 2(c), the position of cassava starch hump 2θ is 15° , 17° , 18° , and 23° , which belongs to type A crystalline starch with a relatively compact structure, and most plant root starch is type A.

As shown in Figure 3, the HCS-ZnO nanoparticle coating had more bubble structure than HCS coating material, which may be due to the stable bubble structure formed by the three-phase material during drying [46]. The bubble structure of the HCS-ZnO nanoparticle coating is beneficial

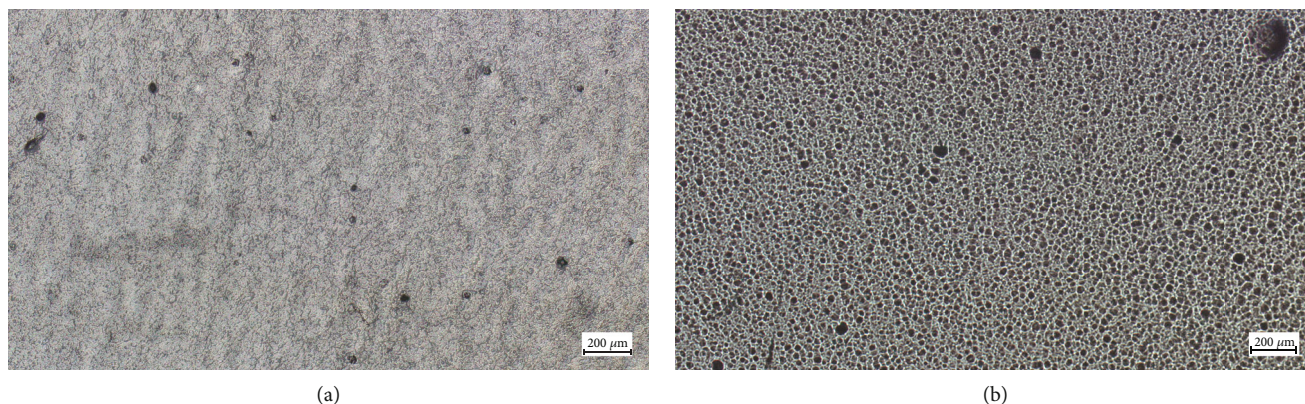


FIGURE 3: Scanning electron microscopic view of (a) cassava starch and (b) cassava starch 0.2% ZnO nanoparticles.

TABLE 1: Weight loss in passion fruit over the storage periods.

Storage at 4°C	Cassava-starch ZnO coating				
	Control (0%)	0.2%	0.4%	0.6%	0.8%
7 (d)	7.30 ± 0.06 ^{A,f}	6.50 ± 0.06 ^{B,f}	7.30 ± 0.10 ^{A,f}	7.40 ± 0.30 ^{A,f}	6.30 ± 0.20 ^{B,f}
14 (d)	14.63 ± 0.28 ^{AB,e}	15.30 ± 0.25 ^{A,e}	14.14 ± 0.23 ^{B,e}	11.95 ± 0.80 ^{C,e}	10.60 ± 0.21 ^{D,e}
21 (d)	21.82 ± 0.38 ^{A,d}	21.46 ± 0.34 ^{A,d}	19.63 ± 0.42 ^{B,d}	17.19 ± 0.78 ^{C,d}	15.73 ± 0.78 ^{C,d}
28 (d)	29.36 ± 0.27 ^{A,c}	28.17 ± 0.28 ^{A,c}	26.21 ± 0.57 ^{B,c}	23.17 ± 1.01 ^{C,c}	20.60 ± 0.96 ^{D,c}
35 (d)	37.31 ± 0.68 ^{A,b}	35.20 ± 0.67 ^{AB,b}	33.41 ± 0.86 ^{B,b}	29.51 ± 1.12 ^{C,b}	26.21 ± 0.79 ^{D,b}
42 (d)	46.68 ± 0.92 ^{A,a}	42.80 ± 0.91 ^{B,a}	40.48 ± 0.79 ^{BC,a}	38.65 ± 1.02 ^{C,a}	33.65 ± 0.92 ^{D,a}

Data presented as mean ± std. Different capital superscript letters in the same row indicate significant differences, while different small superscript letters in the same column indicate significant differences.

to the aerobic respiration of fruits and vegetables, reducing the toxicity of anaerobic respiration to better preserve the quality of fruits and vegetables. In addition to that, nanoparticle coating inhibits the growth of microorganisms present on the surface of fruits and vegetables, inhibiting their reproduction and extending their storage period [47]. The porous structure of the developed coating showed improved compatibility compared to previous findings [48].

3.2. Rate of Weight Loss. Following harvest, passion fruit experiences a decline in water content due to transpiration and respiration processes, which significantly impacts its postharvest quality. Table 1 demonstrates that throughout the storage period, weight loss of passion fruit gradually increased over time. However, when compared to both the control group and other treated samples, passion fruit treated with 0.8% HCS-ZnO nanoparticles exhibited the lowest weight loss rate. This observation may be attributed to the comparatively lower moisture permeability of the 0.8% HCS-ZnO nanoparticle coating. By the end of the storage period, the total weight loss among the five different treatments ranged from 33.7% to 46.7% (Table 1); passion fruit treated with 0.2%, 0.4%, 0.6%, and 0.8% HCS-ZnO nanoparticle composite coating showed 4%, 6%, 8%, and 13% lower weight loss than that of the control group, respectively. These findings underscore the potential for delaying the reduction in weight loss of yellow passion fruit by

employing HCS-ZnO nanoparticle composite coating [49]. Similar results were reported for mangoes coated with carrageenan in combination with ZnO nanoparticles [50]. However, in all cases, the trend of weight loss continues at a constant rate throughout the storage period. This indicates the HCS-ZnO nanoparticle composite coating exhibited constant physical properties, and its porous structure did not make any barrier for water transpiration through the peel. Porous structures were suitable for maintaining the quality since nonporous coatings completely prevent moisture and gas exchange [21, 51].

3.3. Changes in Passion Fruit Peel Color. The visual color changes among different treatments are presented in Figure 4. Changes in L^* , a^* , and b^* values provide significant information regarding the color attributes of passion fruit. L^* values reflect changes in the general brightness of the passion fruit peel. With fruit ripening, the L^* value of passion fruit peel increased at the beginning and decreased gradually (Table 2). L^* value of the control group decreased by 8.44% after 42 days of storage, while 0.2% and 0.6% HCS-ZnO nanoparticle composite coating treatments led to a 0.4% and 2.02% increase, respectively. However, there were no significant ($p > 0.05$) differences in L^* values between the experimental group and the control group.

The a^* value evaluates color along the red-green spectrum, with negative values suggesting green tones. a^* value



FIGURE 4: Visual comparison of control and coated passion fruits within 42 days of storage.

of yellow passion fruit on the day of harvesting was -6.5. During 42 days of storage, the a^* value of all passion fruit increased gradually, rising to 5.8, 1, -0.27, 0.73, and 0.2 after 42 days of storage in the control, 0.2%, 0.4%, 0.6%, and 0.8% HCS-ZnO nanoparticle composite coating treatment, respectively. These results showed that passion fruit peel color became more reddish with storage. During the storage period, no significant ($p < 0.05$) difference was observed between the experimental group and the control group before 35 days of storage, and no significant ($p < 0.05$) difference found in the a^* value between the passion fruit coated with 0.2%, 0.4%, and 0.6% HCS-ZnO nanoparticle coating treated groups. These results are in accordance with the previous study [22].

The b^* value assesses color along the yellow-blue spectrum, with positive values indicating yellow hues. Yellow tones are characteristic of ripe passion fruit. As can be seen from Table 2, the b^* value of passion fruit in all groups showed a rapid downward trend during 7 days of storage and then increased and showed a steady downward trend with the increased storage time. At 35 days of storage, no significant ($p < 0.05$) difference was observed between the HCS-ZnO nanoparticle composite coating treatment and

the control group. The variation trend of L^* , a^* , and b^* values of peel during storage was similar to the previous results of Yumbya et al. [52]. During 7-42 days of storage, the L^* and b^* values of passion fruit decreased with storage time, indicating that the brightness and yellowness degrees of the peel color of the experimental group and the control group decreased with storage time, while the degree of redness of the peel increased. Generally, consumers prefer passion fruits exhibiting vivid yellow colors, as they associate such hues with sweetness and ripeness. The color results showed that the effect of 0.2% HCS-ZnO nanoparticle coating on passion fruit was better, and the peel had a higher L^* value and lower a^* and b^* values.

3.4. Changes in Titrable Acid Content. Titrable acid content of passion fruit plays a crucial role in consumer preference and serves as a marker for fruit ripeness. It influences the perceived tartness of fruits, and a decline in total acidity can diminish the characteristic acidity typically associated with passion fruit. This alteration in acidity levels may affect the overall flavor profile, potentially resulting in a less pronounced tanginess [8, 24]. Titrable acidity tends to decrease during postharvest storage as organic acids are utilized as

TABLE 2: Peel color changes in passion fruits during the storage.

Color parameters	Cassava-starch ZnO coating ZnO content	Storage at 4 °C						
		0 (d)	7 (d)	14 (d)	21 (d)	28 (d)	35 (d)	42 (d)
a^*	0%	-6.53 ± 2.09^a	-4.53 ± 3.23^a	-5.73 ± 5.54^a	0.13 ± 4.10^a	-0.97 ± 6.1^a	5.17 ± 0.85^a	5.10 ± 5.80^a
	0.2%	-6.53 ± 2.09^a	-5.37 ± 2.38^a	-4.93 ± 3.44^a	-3.30 ± 3.22^a	-2.50 ± 4.22^a	-0.87 ± 2.82^a	1.00 ± 5.31^{ab}
	0.4%	-6.53 ± 2.09^a	-5.93 ± 4.27^a	-2.83 ± 4.38^a	-3.80 ± 4.78^a	-2.27 ± 4.26^a	-0.50 ± 0.78^a	-0.27 ± 0.76^{ab}
	0.6%	-6.53 ± 2.09^a	-6.93 ± 6.94^a	-5.00 ± 6.50^a	-5.47 ± 6.81^a	-4.10 ± 6.10^a	-1.70 ± 5.89^a	0.73 ± 3.67^{ab}
	0.8%	-6.53 ± 2.09^a	-6.93 ± 1.80^a	-6.13 ± 4.19^a	-6.07 ± 4.04^a	-5.13 ± 6.36^a	-4.37 ± 8.03^a	0.20 ± 6.65^b
b^*	0%	39.00 ± 1.87^a	34.83 ± 5.76^a	39.63 ± 3.39^a	39.33 ± 2.49^a	38.70 ± 1.56^a	39.00 ± 1.85^a	37.87 ± 0.67^{ab}
	0.2%	39.00 ± 1.87^a	36.93 ± 5.30^a	38.63 ± 3.66^a	40.01 ± 1.05^a	37.47 ± 3.40^a	37.37 ± 8.21^a	40.13 ± 2.15^a
	0.4%	39.00 ± 1.87^a	37.30 ± 0.57^a	41.10 ± 6.01^a	40.60 ± 3.28^a	37.40 ± 5.09^a	41.07 ± 3.40^a	39.77 ± 4.38^a
	0.6%	39.00 ± 1.87^a	30.57 ± 5.28^a	38.60 ± 3.36^a	36.77 ± 4.23^a	37.13 ± 3.52^a	37.50 ± 2.52^a	37.83 ± 1.50^{ab}
	0.8%	39.00 ± 1.87^a	28.73 ± 5.40^a	37.47 ± 2.82^a	37.13 ± 4.84^a	37.50 ± 1.81^a	36.37 ± 1.15^a	32.97 ± 4.18^a
L^*	0%	59.23 ± 2.79^a	63.00 ± 5.90^a	58.10 ± 7.13^a	58.27 ± 7.79^a	57.87 ± 5.06^a	58.27 ± 2.57^a	54.23 ± 4.46^a
	0.2%	59.23 ± 2.79^a	65.27 ± 7.68^a	64.90 ± 8.76^a	65.10 ± 3.27^a	62.03 ± 14.25^a	55.2 ± 14.27^a	59.47 ± 5.46^a
	0.4%	59.23 ± 2.79^a	69.00 ± 3.40^a	68.77 ± 5.34^a	62.73 ± 7.35^a	54.57 ± 9.77^a	56.03 ± 7.45^a	52.80 ± 4.52^a
	0.6%	59.23 ± 2.79^a	64.00 ± 7.05^a	62.20 ± 7.91^a	58.23 ± 7.05^a	56.06 ± 8.44^a	57.10 ± 7.06^a	60.43 ± 11.89^a
	0.8%	59.23 ± 2.79^a	67.17 ± 5.41^a	60.87 ± 2.68^a	59.80 ± 8.25^a	59.27 ± 5.62^a	56.17 ± 5.32^a	55.60 ± 3.14^a

Note: data are means \pm standard deviation ($N = 3$ for both control samples and treated samples). Means followed by different letters within the column at each week indicate significant differences between the treatments according to Tukey's HSD test at $p = 0.05$.

primary substrates for respiration and other metabolic activities. It can be seen from Figure 5 that during storage, the total acid content of passion fruit showed a downward trend, mainly because organic acids in fruits and vegetables are major respiratory substrates, the main source of ATP, and the providers of intermediate metabolites required by essential cellular biochemical processes [5, 53]. Throughout the storage duration, the overall acid content of passion fruit exhibited a gradual decline. This phenomenon stems from the ripening process of passion fruit, where the sucrose content diminishes, subsequently leading to reductions in fructose and glucose levels. During the initial stages of ripening, there was a slight increase in citric acid and malic acid content, followed by a subsequent decrease, resulting in relatively stable changes in titratable acidity. Over the storage period, a significant difference ($p < 0.05$) in total acid content was observed between the treated and control samples. Notably, passion fruits treated with a 0.2% HCS-ZnO nanoparticle coating experienced a decrease in total acid content by only 0.95 g/100 mL, a significantly ($p < 0.05$) smaller reduction compared to the control group at 42 days. This finding suggests that the metabolism within passion fruit may be attenuated at this concentration. It is plausible that the HCS-ZnO coating inhibited the respiratory process of passion fruit, thereby mitigating the decline rate of total acid content in the fruit.

3.5. Changes in Total Soluble Solid Content (TSS). The ratio of TSS to total titratable acidity, reflecting the equilibrium between sugar and acid levels, plays a pivotal role in determining the aroma and taste profile of the passion fruit. A higher ratio typically denotes a sweeter flavor profile, while a lower ratio suggests higher acidity. Fruit palatability is

strongly associated with the above-mentioned ratio, as consumers generally favor passion fruits that exhibit a harmonious balance of sweetness and acidity [7, 23]. Hence, TSS is an important indicator during storage. Changes in TSS content are a reflection of fruit maturity and respiration. The TSS content of passion fruit during cold storage increased gradually (Figure 6) in both the experimental group and the control group. The rise in TSS can be attributed to the decomposition of starch into sugar, CO_2 , and water, as well as the hydrolysis of cell wall polysaccharides and water loss, which resulted in an increase in dry matter. During the later storage period, TSS content fluctuated due to individual differences [54]. Among the four treatment groups, the TSS content of the 0.2% HCS-ZnO nanoparticle composite coating treated group was relatively stable and significantly ($p < 0.05$) lower than that of the other groups. This result is in accordance with that of the earlier work [55, 56].

3.6. Changes in Electrical Conductivity. During the storage, as shown in Figure 7, the electrical conductivity of each treated group increased gradually, indicating that the integrity of the cell membrane of passion fruit changed during storage. During passion fruit storage, the senescence of fruit cells increased the membrane permeability, which increased the electrolyte leakage from fruit flesh and increased the relative conductivity, and thus, the degree of cell injury was represented by the phase conductivity [57]. At the beginning of storage, the control group showed a lower value of electrical conductivity than the 0.8% HCS-ZnO-treated groups. This result might be due to the fact that treatments accelerated the early metabolism of passion fruit, which promoted cytoplasmic lysis [58]. It can be seen from Figure 7 that conductivity fluctuated during storage. This phenomenon

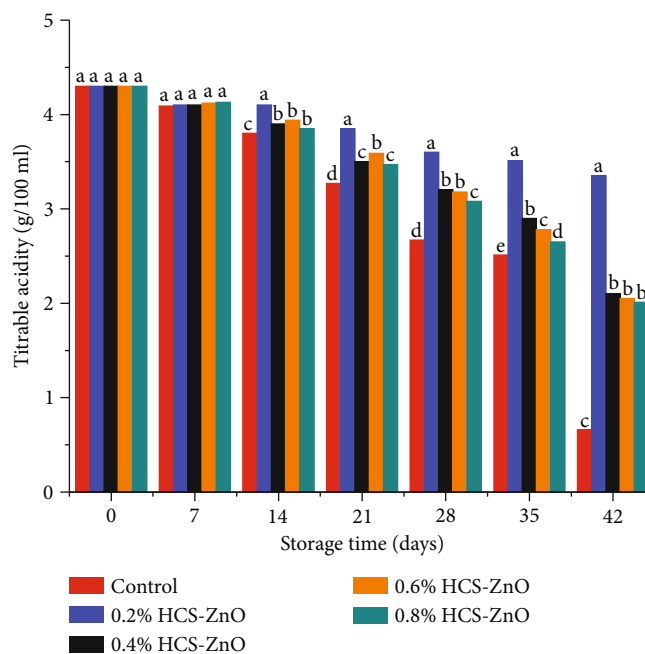


FIGURE 5: Changes in titratable acidity of passion fruit during storage. Means followed by different letters within the figure at different sampling days indicate significant differences between the treatments according to Tukey's HSD test at $p = 0.05$.

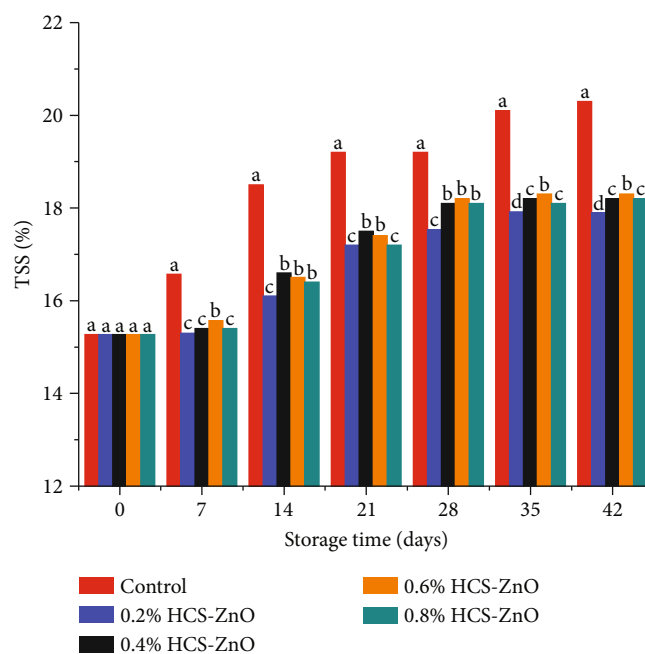


FIGURE 6: Changes in the soluble solids content of passion fruit during storage. Means followed by different letters within the figure at different sampling days indicate significant differences between the treatments according to Tukey's HSD test at $p = 0.05$.

suggests that there was an interaction of substances that retarded the fluidization of the cytoplasm [59]. Compared with the control group, the electrical conductivity of passion fruit treated with HCS-ZnO nanoparticle coating was significantly lower ($p < 0.05$), indicating that the integrity of the cell membrane was better maintained and had little effect on passion fruit metabolism.

3.7. Changes in Reducing Sugar Content. Reducing sugar is one of the sources of fruit sweetness, and its content is among the main indicators of fruit ripeness. After 42 days of storage, as shown in Figure 8, the content of reducing sugar was 6.2, 5.1, 5.6, 5.64, and 5.5 g/100 g in the control group 0.2%, 0.4%, 0.6%, and 0.8% HCS-ZnO nanoparticle-treated groups, respectively. During storage with the metabolic

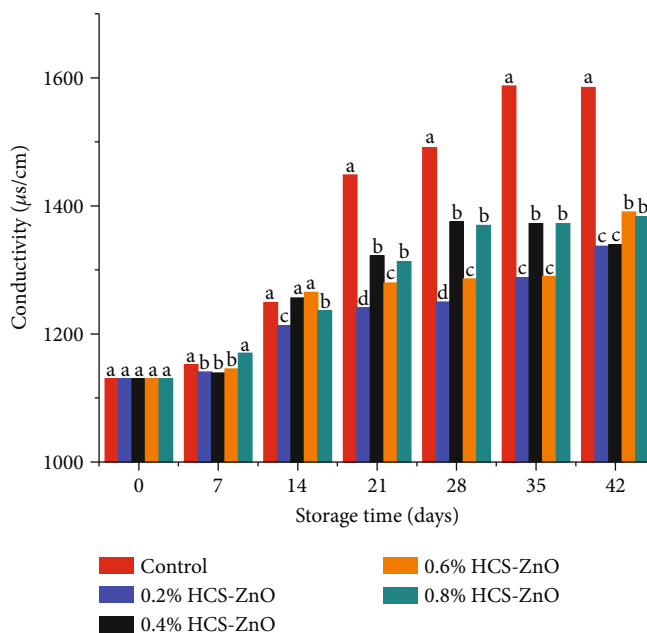


FIGURE 7: Changes in electrical conductivity ($\mu\text{s}/\text{cm}$) in the preservation of passion fruit during storage. Means followed by different letters within the figure at different sampling days indicate significant differences between the treatments according to Tukey's HSD test at $p = 0.05$.

processes, organic matter decomposed into simple metabolites, or large starch hydrolyzed and converted into small sugar molecules, resulting in a peak of reducing sugar and soluble solids content. In the current experiment, at 42 days of storage, the reducing sugar content of passion fruit treated with 0.2% HCS-ZnO nanoparticle coating showed the lowest value of 5.1 g/100 g, which was significantly ($p < 0.05$) lower than that of the control group and other treatment groups. The compound coating treatment at this concentration could effectively maintain the reducing sugar content [60].

3.8. Principal Component Analysis. Principal component analysis (PCA) analysis provides an overview of the data and reduces the dimensions of the data. Since PCA represents the data with fewer number of latent variables, also known as principal components (PCs), it is easier to understand and explore the relationships among/between variables and samples [5]. The result of PCA is shown in Figure 9. Two PCs were chosen while constructing the PCA where the first PC contributed 73% and the second PC contributed 13% of the variation. Moreover, an additional PC could not provide clearer clusters of samples. It can be seen from the score plot that samples with different treatments on different days of evaluation made small clusters (Figure 9(a)). The most variation observed among the samples was on day 7 and on day 42. An interesting trend can be observed from the PCA score plot that samples moved from left to right with the increase in storage days. From the loading plot, it can be observed that samples were high in acidity, and with time, acidity decreased and other parameters increased (Figure 9(b)). Samples treated with 0.8% HCS-ZnO nanoparticles attributed to higher lightness, while samples treated with 0.4% HCS-ZnO nanoparticles attributed to a more yellowish color.

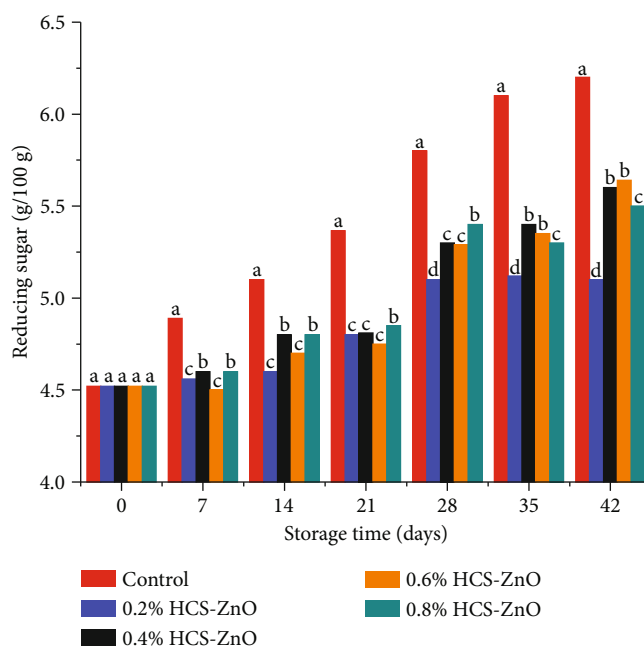


FIGURE 8: Effects of different treatments on reducing sugar content of passion fruit. Means followed by different letters within the figure at different sampling days indicate significant differences between the treatments according to Tukey's HSD test at $p = 0.05$.

While the current investigation revealed several intriguing advantages of employing an HCS-ZnO nanoparticle coating on passion fruits, certain limitations remain within this study. A proper investigation is required to assess whether any components of the HCS-ZnO nanoparticles migrate from the coating onto the passion fruit during

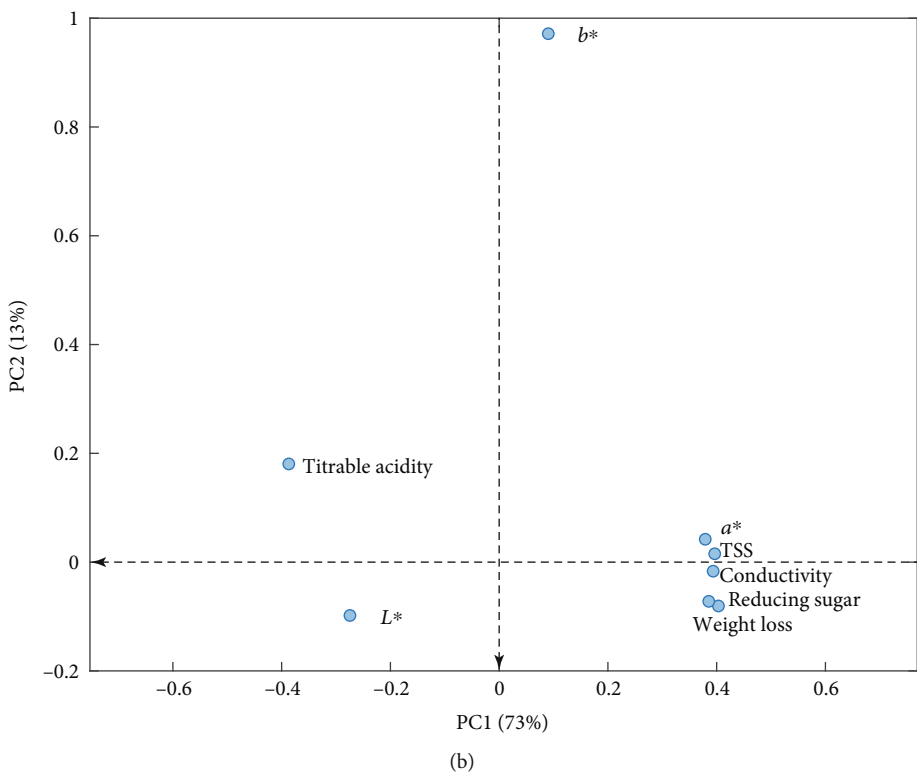
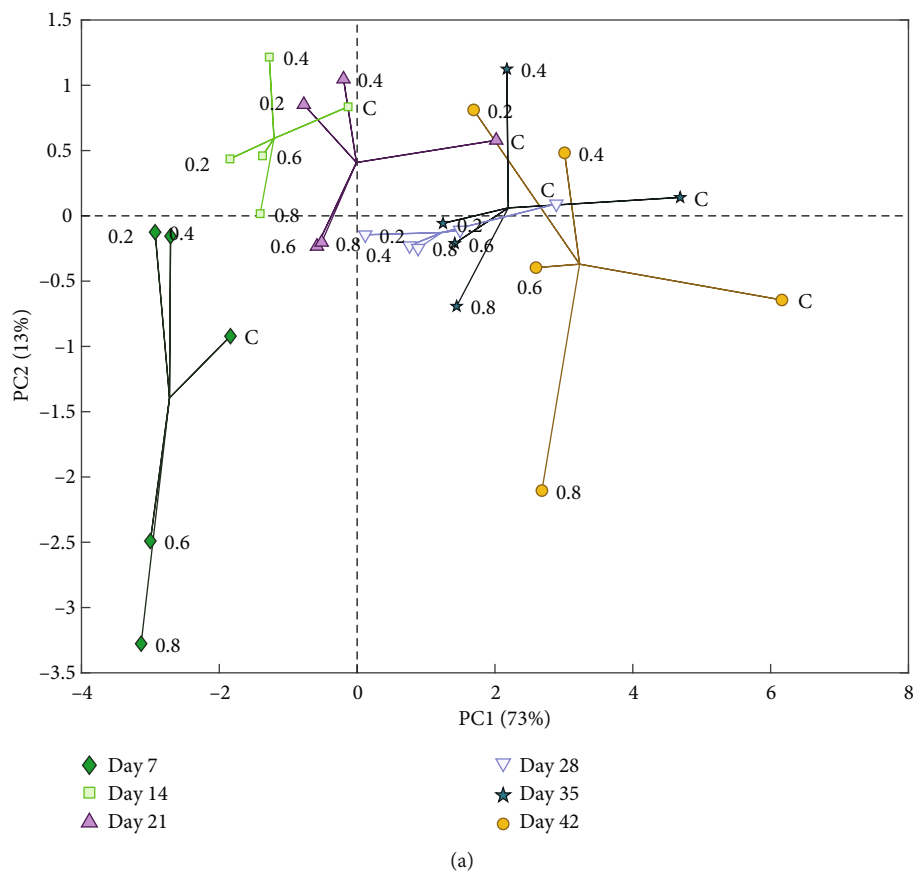


FIGURE 9: PCA score (a) and loading (b) plot of the samples. Samples in the score plot marked according to the HCS-ZnO percentage.

storage or handling, aiming to assess the safety and stability of the coating, ensuring that it does not introduce any harmful substances onto the fruit. This information would help the technology be adopted in commercial settings. Moreover, measuring the thickness of the coating would provide clear understanding of the gas and moisture permeability and uniformity of the coating. In addition, for better understanding of the physiological process and interactions/additive effects, the effect of the coating on respiration rate as well as individual control study should be carried out in future study.

4. Conclusion

In this study, the micromorphology of the HCS-ZnO nanoparticle coating was evaluated, and its effects on passion fruit preservation were studied. It was found that the HCS-ZnO nanoparticle coating forms a homogeneous porous structure on the surface of passion fruit. This novel treatment was found to reduce water and nutrition loss in passion fruit and alleviate deterioration of quality during storage. Comparing all the treatments, it can be concluded that 0.2% HCS-ZnO nanoparticle coating maintained the total soluble solids, total acids, and cell membrane permeability and reduced the loss of passion fruit nutrients during storage. Future study could involve further exploration and optimization of the HCS-ZnO nanoparticle coating for other climacteric fruit preservation. Additionally, there could be deeper investigations into the potential cytotoxicity and related health risks.

Data Availability

The data that support the findings of this study are available on request from the corresponding author. The data are not publicly available due to privacy or ethical restrictions.

Disclosure

The funders had no role in the study design, data collection and analysis, decision to publish, or preparation of the manuscript.

Conflicts of Interest

On behalf of all authors, the corresponding author states that there is no conflict of interest (between the corresponding author and the co-authors).

Authors' Contributions

Han Congying was responsible for the conceptualization, funding acquisition, experiment, writing the original manuscript, and writing-review-editing; Wang Meifang was responsible for the experiment and data curing; Md. Nahidul Islam was responsible for the conceptualization, experiment, supervision, formal analysis, data curing, data analysis, writing the original manuscript, writing-review-editing, and funding acquisition; Shi Cancan was responsible for the experiment and visualization; Guo Shengli was responsible

for the writing-review-editing; Afsana Hossain was responsible for the writing-review-editing; Cao Xiaohuang was responsible for the funding acquisition, supervision, data analysis, and writing the original manuscript.

Acknowledgments

The authors acknowledge the financial support from the Yulin Normal University Start Fund (2020ZK08), the Guangxi Key Research and Development Plan (2018AB45026), the Middle-aged and young teachers' project Basic ability Promotion of Guangxi (2020KY14017), the Ministry of Science and Technology, Peoples Republic of Bangladesh (SRG-221157), the University Grants Commission of Bangladesh (Project # CropScience-09/2021-2022), and the Yulin science technology project plan (20220514).

References

- [1] X. He, F. Luan, Y. Yang et al., "Passiflora edulis: an insight into current researches on phytochemistry and pharmacology," *Frontiers in Pharmacology*, vol. 11, p. 617, 2020.
- [2] X.-N. Xing, Y.-C. Huang, G. Chen et al., "Current status, existing problems and development suggestions of Guangxi passion fruit industry," *Journal of Southern Agriculture*, vol. 51, no. 5, pp. 1240–1246, 2020.
- [3] K. Kishore, K. A. Pathak, R. Shukla, and R. Bharali, "Effect of storage temperature on physico-chemical and sensory attributes of purple passion fruit (*Passiflora edulis* Sims)," *Journal of Food Science and Technology*, vol. 48, no. 4, pp. 484–488, 2011.
- [4] A. Pongener, V. Sagar, R. K. Pal, R. Asrey, R. R. Sharma, and S. K. Singh, "Physiological and quality changes during post-harvest ripening of purple passion fruit (*Passiflora edulis* Sims)," *Fruits*, vol. 69, no. 1, pp. 19–30, 2014.
- [5] M. S. Mahomud, M. N. Islam, and J. Roy, "Effect of low oxygen stress on the metabolic responses of tomato fruit cells," *Heliyon*, vol. 10, no. 3, article e24566, 2024.
- [6] S. Ahmed, S. Akther, S. M. S. Alam, M. Ahiduzzaman, M. N. Islam, and M. S. Azam, "Individual and combined effects of electrolyzed water and ultrasound treatment on microbial decontamination and shelf life extension of fruits and vegetables: a review of potential mechanisms," *Journal of Food Processing and Preservation*, vol. 46, no. 8, Article ID e16765, 2022.
- [7] P. Ezati, J.-W. Rhim, R. Molaei, R. Priyadarshi, and S. Han, "Cellulose nanofiber-based coating film integrated with nitrogen-functionalized carbon dots for active packaging applications of fresh fruit," *Postharvest Biology and Technology*, vol. 186, article 111845, 2022.
- [8] L. Huang, D.-W. Sun, H. Pu, C. Zhang, and D. Zhang, "Nanocellulose-based polymeric nanozyme as bioinspired spray coating for fruit preservation," *Food Hydrocolloids*, vol. 135, article 108138, 2023.
- [9] P. Qu, M. Zhang, K. Fan, and Z. Guo, "Microporous modified atmosphere packaging to extend shelf life of fresh foods: a review," *Critical Reviews in Food Science and Nutrition*, vol. 62, no. 1, pp. 51–65, 2022.
- [10] M. N. Islam, A. Wang, J. S. Pedersen, J. N. Sørensen, O. Körner, and M. Edelenbos, "Online measurement of temperature and relative humidity as marker tools for quality

- changes in onion bulbs during storage,” *PLoS One*, vol. 14, no. 1, article e0210577, 2019.
- [11] D.-K. Liu, C.-C. Xu, C.-X. Guo, and X.-X. Zhang, “Sub-zero temperature preservation of fruits and vegetables: a review,” *Journal of Food Engineering*, vol. 275, article 109881, 2020.
- [12] J. B. Dutra, L. E. B. Blum, L. F. Lopes, A. F. Cruz, and C. H. Uesugi, “Use of hot water, combination of hot water and phosphite, and 1-MCP as post-harvest treatments for passion fruit (*Passiflora edulis* f. *flavicarpa*) reduces anthracnose and does not alter fruit quality,” *Horticulture, Environment, and Biotechnology*, vol. 59, no. 6, pp. 847–856, 2018.
- [13] M. F. Dewan, M. N. Islam, and M. S. Azam, “Food additives/preservatives and their implications for human health,” in *Food Safety*, pp. 155–184, CRC Press, 2024.
- [14] P. K. Raghav, N. Agarwal, and M. Saini, “Edible coating of fruits and vegetables: a review,” *Education*, vol. 1, pp. 2455–5630, 2016.
- [15] C. Xiaohuang, H. Qianqian, Y. Cong, M. S. Azam, M. Ahiduzzaman, and M. N. Islam, “Enhancement of the selected physico-chemical properties of steamed rice cake by the application of acetylated distarch adipate,” *Journal of Food Measurement and Characterization*, vol. 16, no. 5, pp. 3526–3536, 2022.
- [16] M. M. Marvizadeh, N. Oladzadabbasabadi, A. Mohammadi Nafchi, and M. Jokar, “Preparation and characterization of bionanocomposite film based on tapioca starch/bovine gelatin/nanorod zinc oxide,” *International Journal of Biological Macromolecules*, vol. 99, pp. 1–7, 2017.
- [17] FDA, *Select Committee on GRAS Substances (SCOGS) Opinion: Zinc Salts 2015*, Food and Drug Administration, Washington DC, USA, 2010, April 2024, <https://www.accessdata.fda.gov/scripts/cdrh/cfdocs/cfcfr/CFRSearch.cfm?fr=182.8991>.
- [18] S. Iuliani, A. A. Wardana, B. Meindrawan, N. Edhi, and T. R. Muchtadi, “Nanocomposite edible coating from cassava starch, stearic acid and ZnO nanoparticles to maintain quality of fresh-cut mango cv. Arumanis,” *The Annals of the University Dunarea De Jos of Galati. Fascicle VI-Food Technology*, vol. 42, no. 2, pp. 49–58, 2018.
- [19] D. D. La, P. Nguyen-Tri, K. H. le et al., “Effects of antibacterial ZnO nanoparticles on the performance of a chitosan/gum arabic edible coating for post-harvest banana preservation,” *Progress in Organic Coatings*, vol. 151, article 106057, 2021.
- [20] K. H. Le, M. D. B. Nguyen, L. D. Tran et al., “A novel antimicrobial ZnO nanoparticles-added polysaccharide edible coating for the preservation of postharvest avocado under ambient conditions,” *Progress in Organic Coatings*, vol. 158, article 106339, 2021.
- [21] T. Odetayo, S. Tesfay, and N. Z. Ngobese, “Nanotechnology-enhanced edible coating application on climacteric fruits,” *Food Science & Nutrition*, vol. 10, no. 7, pp. 2149–2167, 2022.
- [22] J. R. dos Santos Junior, L. C. Corrêa-Filho, V. O. Pereira et al., “Application of rosin resin and zinc oxide nanocomposites to chitosan coatings for extending the shelf life of passion fruits,” *Sustainable Food Technology*, vol. 2, no. 2, pp. 415–425, 2024.
- [23] A. Galindez, L. D. Daza, A. Homez-Jara, A. Sandoval-Aldana, and H. A. Váquiro, “Effect of ulluco starch coating on the preservation of harvested goldenberries (*Physalis peruviana* L.),” *Journal of Food Processing and Preservation*, vol. 45, no. 12, Article ID e16071, 2021.
- [24] M. C. G. Pellá, O. A. Silva, M. G. Pellá et al., “Effect of gelatin and casein additions on starch edible biodegradable films for fruit surface coating,” *Food Chemistry*, vol. 309, article 125764, 2020.
- [25] N. Tamimi, A. Mohammadi Nafchi, H. Hashemi-Moghadam, and H. Baghaie, “The effects of nano-zinc oxide morphology on functional and antibacterial properties of tapioca starch bionanocomposite,” *Food Science & Nutrition*, vol. 9, no. 8, pp. 4497–4508, 2021.
- [26] M. Zare, K. Namratha, K. Byrappa, D. M. Surendra, S. Yallappa, and B. Hungund, “Surfactant assisted solvothermal synthesis of ZnO nanoparticles and study of their antimicrobial and antioxidant properties,” *Journal of Materials Science & Technology*, vol. 34, no. 6, pp. 1035–1043, 2018.
- [27] T. Phinainitisatra and N. Harnkarnsujarit, “Development of starch-based peelable coating for edible packaging,” *International Journal of Food Science & Technology*, vol. 56, no. 1, pp. 321–329, 2021.
- [28] J. Zhu, W. Gao, B. Wang et al., “Preparation and evaluation of starch-based extrusion-blown nanocomposite films incorporated with nano-ZnO and nano-SiO₂,” *International Journal of Biological Macromolecules*, vol. 183, pp. 1371–1378, 2021.
- [29] W. Schotsmans and G. Fischer, “Passion fruit (*Passiflora edulis* Sim.),” in *Postharvest biology and technology of tropical and subtropical fruits*, pp. 125–143e, Elsevier, 2011.
- [30] A. C. Janaki, E. Sailatha, and S. Gunasekaran, “Synthesis, characteristics and antimicrobial activity of ZnO nanoparticles,” *Spectrochimica Acta. Part A, Molecular and Biomolecular Spectroscopy*, vol. 144, pp. 17–22, 2015.
- [31] C. Karpagasundari and S. Kulothungan, “Analysis of bioactive compounds in *Physalis minima* leaves using GC MS, HPLC, UV-VIS and FTIR techniques,” *Journal of Pharmacognosy and Phytochemistry*, vol. 3, no. 4, pp. 196–201, 2014.
- [32] M. N. Rahman, M. N. Islam, M. M. Mia, S. Hossen, M. F. Dewan, and M. S. Mahomud, “Fortification of set yoghurts with lemon peel powders: an approach to improve physico-chemical, microbiological, textural and sensory properties,” *Applied Food Research*, vol. 4, no. 1, article 100386, 2024.
- [33] X. Cao, M. N. Islam, X. Ning, Z. Luo, and L. Wang, “Effects of superheated steam processing on the physicochemical properties of sea rice bran,” *Food Science and Technology International*, vol. 29, no. 2, pp. 115–125, 2023.
- [34] W. Zhou, X. Cao, M. N. Islam et al., “Comparison of hydrability, antioxidants, microstructure, and sensory quality of barley grass powder using ultra-micro-crushing combined with hot air and freeze drying,” *Food Science & Nutrition*, vol. 9, no. 4, pp. 1870–1880, 2021.
- [35] S. Alam, M. Ahiduzzaman, M. N. Islam, M. A. Haque, and M. A. M. Akanda, “Formulation and senso-chemical evaluation of aloe vera (*Aloe barbadensis* Miller) based value added beverages,” *Annals of Bangladesh Agriculture*, vol. 25, no. 1, pp. 43–54, 2022.
- [36] M. N. Islam, M. Zhang, B. Adhikari, C. Xinfeng, and B. G. Xu, “The effect of ultrasound-assisted immersion freezing on selected physicochemical properties of mushrooms,” *International Journal of Refrigeration*, vol. 42, pp. 121–133, 2014.
- [37] G. L. Miller, “Use of dinitrosalicylic acid reagent for determination of reducing sugar,” *Analytical Chemistry*, vol. 31, no. 3, pp. 426–428, 1959.
- [38] M. A. Ali, K. K. Saha, M. S. Choudhury, M. Ahiduzzaman, and M. N. Islam, “Formulation, senso-chemical analysis and shelf-life study of biscuits using stevia leaf as the substitute for

- sugar," *Asian Journal of Dairy and Food Research*, vol. 41, no. 4, pp. 424–430, 2022.
- [39] L. G. Dias, A. P. Pereira, and L. M. Estevinho, "Comparative study of different Portuguese samples of propolis: pollinic, sensorial, physicochemical, microbiological characterization and antibacterial activity," *Food and Chemical Toxicology*, vol. 50, no. 12, pp. 4246–4253, 2012.
- [40] M. M. Hasan, Ahiduzzaman, N. Islam, A. Haque, and M. Hossain, "Formulation and senso-chemical evaluation of palmyrah palm (*Borassus flabellifer* L.) based value-added products," *Journal of Food Research*, vol. 11, no. 3, p. 36, 2022.
- [41] M. N. Islam, "Chemometrics in nondestructive quality evaluation," in *Nondestructive quality assessment techniques for fresh fruits and vegetables*, pp. 331–355, Springer, 2022.
- [42] R. Hong, J. H. Li, L. L. Chen et al., "Synthesis, surface modification and photocatalytic property of ZnO nanoparticles," *Powder Technology*, vol. 189, no. 3, pp. 426–432, 2009.
- [43] S. O. Ogunyemi, Y. Abdallah, M. Zhang et al., "Green synthesis of zinc oxide nanoparticles using different plant extracts and their antibacterial activity against *Xanthomonas oryzae* pv. *oryzae*," *Artificial Cells, Nanomedicine, and Biotechnology*, vol. 47, no. 1, pp. 341–352, 2019.
- [44] R. Lian, J. Cao, X. Jiang, and A. V. Rogachev, "Physicochemical, antibacterial properties and cytocompatibility of starch/chitosan films incorporated with zinc oxide nanoparticles," *Materials Today Communications*, vol. 27, article 102265, 2021.
- [45] Z. H. Stachurski, "On structure and properties of amorphous materials," *Materials*, vol. 4, no. 9, pp. 1564–1598, 2011.
- [46] X. Cao, W. Xu, and M. N. Islam, "Impact of different drying methods on physicochemical characteristics and nutritional compositions of bee larvae," *Drying Technology*, vol. 42, pp. 1–14, 2024.
- [47] W. Hu, Z. Zou, H. Li, Z. Zhang, J. Yu, and Q. Tang, "Fabrication of highly transparent and multifunctional polyvinyl alcohol/starch based nanocomposite films using zinc oxide nanoparticles as compatibilizers," *International Journal of Biological Macromolecules*, vol. 204, pp. 284–292, 2022.
- [48] V. Pitpisutkul and J. Prachayawarakorn, "Hydroxypropyl methylcellulose/carboxymethyl starch/zinc oxide porous nanocomposite films for wound dressing application," *Carbohydrate Polymers*, vol. 298, article 120082, 2022.
- [49] M. Islam, M. Alam, M. Amin, and D. Roy, "Effect of sun drying on the composition and shelf life of goat meat (*Capra aegagrus hircus*)," *Bangladesh Research Publications Journal*, vol. 4, no. 2, pp. 114–123, 2010.
- [50] B. Meindrawan, N. E. Suyatma, A. A. Wardana, and V. Y. Pamela, "Nanocomposite coating based on carrageenan and ZnO nanoparticles to maintain the storage quality of mango," *Food Packaging and Shelf Life*, vol. 18, pp. 140–146, 2018.
- [51] F. Rezaei and Y. Shahbazi, "Shelf-life extension and quality attributes of sauced silver carp fillet: a comparison among direct addition, edible coating and biodegradable film," *LWT*, vol. 87, pp. 122–133, 2018.
- [52] P. Yumbya, J. Ambuko, S. I. Shibairo, and W. Owino, "Effect of modified atmosphere packaging (MAP) on the shelf life and postharvest quality of purple passion fruit (*passiflora edulis* sims)," *Journal of Postharvest Technology*, vol. 2, no. 1, pp. 025–036, 2014.
- [53] D. Jianglian, "Application of chitosan based coating in fruit and vegetable preservation: a review," *Journal of Food Processing & Technology*, vol. 4, no. 5, 2013.
- [54] M. Petriccione, F. De Sanctis, M. S. Pasquariello et al., "The effect of chitosan coating on the quality and nutraceutical traits of sweet cherry during postharvest life," *Food and Bioprocess Technology*, vol. 8, no. 2, pp. 394–408, 2015.
- [55] E. Bosquez-Molina and L. Zavaleta-Avejar, "New bioactive biomaterials based on chitosan," in *Chitosan in the Preservation of Agricultural Commodities*, pp. 33–64, Elsevier, 2016.
- [56] W. Lu, L. Bincheng, T. Xiaoyu et al., "Effect of protocatechuic acid-pullulan compound coating on the preservation of post-harvest pepper," *Journal of Nuclear Agricultural Sciences*, vol. 33, no. 4, p. 739, 2019.
- [57] X.-Y. Li, X. L. Du, Y. Liu, L. J. Tong, Q. Wang, and J. L. Li, "Rhubarb extract incorporated into an alginate-based edible coating for peach preservation," *Scientia Horticulturae*, vol. 257, article 108685, 2019.
- [58] B. R. Parry, I. V. Surovtsev, M. T. Cabeen, C. S. O'Hern, E. R. Dufresne, and C. Jacobs-Wagner, "The bacterial cytoplasm has glass-like properties and is fluidized by metabolic activity," *Cell*, vol. 156, no. 1-2, pp. 183–194, 2014.
- [59] L. Wang, C. Hu, and L. Shao, "The antimicrobial activity of nanoparticles: present situation and prospects for the future," *International Journal of Nanomedicine*, vol. 12, pp. 1227–1249, 2017.
- [60] A. K. Yadav and S. V. Singh, "Osmotic dehydration of fruits and vegetables: a review," *Journal of Food Science and Technology*, vol. 51, no. 9, pp. 1654–1673, 2014.